Revista Internacional de Investigación e Innovación Tecnológica

Página principal: www.riiit.com.mx

Influence of $MgFe_2O_4$ on the magnetic properties of glass-Ceramics derived from sol-gel synthesis

Influencia de $MgFe_2O_4$ en las propiedades magnéticas de vitrocerámicas derivadas de la síntesis por sol-gel

De Hoyos-Sifuentes, D.H.[a], Reséndiz-Hernández, P.J.[a]*, García-Cerda, L.A.[b]

[a] División de Estudios de Posgrado e Investigación. Tecnológico Nacional de México/I.T. de Saltillo. 25280. Saltillo, Coahuila. México.

[b] Centro de Investigación en Química Aplicada (CIQA). 25294. Saltillo, Coahuila. México.

d22050002@saltillo.tecnm.mx; perla.rh@saltillo.tecnm.mx*; luis.garcia@ciqa.edu.mx

Technological innovation: synthesis of magnetic glass-ceramics with $MgFe_2O_4$ with bioactive properties.
Area of industrial application: biomedicine, specifically in magnetic hyperthermia treatments and bone regeneration.

Received: january 16th, 2025
Accepted: may 07th, 2025

Resumen

Las vitrocerámicas magnéticas están compuestas por una fase magnética, usualmente un óxido de hierro, integrado en una matriz vítrea. Cuando se utiliza vidrio bioactivo como matriz, estas no solo presentan notables propiedades magnéticas, sino que también adquieren propiedades de bioactividad. Entre los óxidos de hierro, destacan aquellos que incorporan magnesio, un catión esencial en el cuerpo humano, debido a su impacto en varios procesos metabólicos. Esta adición mejora las propiedades de las vitrocerámicas, otorgándoles biocompatibilidad superior, comportamiento magnético blando y eficacia en el calentamiento por inducción, haciéndolas ideales para aplicaciones médicas como la hipertermia magnética.

En este estudio, se sintetizaron mediante sol-gel vitrocerámicas magnéticas con 5, 10, 15 y 20 % peso de $MgFe_2O_4$. Con el objetivo de evaluar el efecto del porcentaje de adición de $MgFe_2O_4$ en las propiedades magnéticas. Los materiales obtenidos fueron caracterizados mediante XRD, FTIR, VSM y TEM. Los análisis por XRD y FTIR evidenciaron la presencia de la fase de $MgFe_2O_4$ y la formación de la fase de hidroxiapatita. Las curvas de histéresis demostraron una magnetización de saturación de 7.95 emu/g en las muestras con 20% de $MgFe_2O_4$. Mediante TEM, se identificaron nanopartículas con morfologías esféricas, con un tamaño promedio de partícula de 6.10 nm.

Palabras clave: Ferritas, $MgFe_2O_4$, Sol-Gel, Vitrocerámicas.

Abstract

Magnetic glass-ceramics are composed of a magnetic phase, usually an iron oxide, integrated in a glass matrix. When bioactive glass is used as the matrix, these materials not only exhibit remarkable magnetic properties**,** but also acquire bioactivity properties. Among iron oxides, those incorporating magnesium, an essential cation in the human body stands out due to their impact on various metabolic processes. This addition enhances the properties of the glass-ceramics, providing superior biocompatibility, superparamagnetic behavior, and efficiency in induction heating, making them ideal for medical applications such as magnetic hyperthermia.

In this study, magnetic glass-ceramics with 5, 10, 15, and 20 wt% of $MgFe_2O_4$ were synthesized using the sol-gel method. In order to evaluate the effect of the percentage of $MgFe_2O_4$ addition on the magnetic properties. The materials obtained were characterized using XRD, FTIR, VSM, and TEM. XRD and FTIR analyses revealed the presence of the $MgFe_2O_4$ phase and the formation of the hydroxyapatite phase. Hysteresis curves demonstrated superparamagnetic behavior, with a saturation magnetization of 7.95 emu/g in the samples containing 20% $MgFe_2O_4$. TEM analysis identified nanoparticles with spherical morphologies, with an average particle size of 6.10 nm.

Keywords: Ferrites, $MgFe_2O_4$, Sol-Gel, Glass-ceramics.

1. Introduction

The synthesis of glass-ceramics using the sol-gel method, particularly when incorporating magnetic components, has opened up new possibilities in the field of regenerative medicine and advanced oncological treatments such, as magnetic hyperthermia. The interest in these materials lies in the unique characteristics they exhibit when bioactive glass is used as a matrix. These glasses, developed by Larry Hench in the 1960s (Hench, 2006), marked a milestone in biomaterials engineering due to their remarkable biocompatibility, osteoconduction, and osteoinduction (Joughehdoust & Manafi, 2012; Shearer et al., 2023). These properties are enhanced in glasses synthesized via the sol-gel method (Farid, 2019), which allows low-temperature synthesis and produces materials with nanometric porosity, facilitating the controlled release of ions, crucial for bone tissue formation. Recent developments have further expanded the capabilities of bioactive glasses by tailoring their degradation rates, improving mechanical properties through innovative scaffold architectures, and incorporating therapeutic ions such as Mg, Cu, Zn, and Sr to promote angiogenesis and enhance tissue regeneration (Kaou et al., 2023; Zhu et al., 2024).

Regarding the magnetic components, the integration of magnesium ferrites into bioactive glass matrices over other ferrites is further justified by several advantages. Magnesium ferrite exhibits lower toxicity profiles, greater chemical stability under physiological conditions, soft magnetic behavior, marked by low coercivity and high saturation magnetization at biomedical operating temperatures (Thompson et al., 2017). These features are particularly desirable for biomedical applications where both biocompatibility and efficient magnetic response are critical. Moreover, the degradation of magnesium ions in vivo does not trigger harmful inflammatory responses, a risk associated with other divalent cations ferrites (Díez-Tercero et al., 2021). Beyond hyperthermia, magnetic glass-ceramics can

also be used in other biomedical applications such as drug delivery systems, where an external magnetic field guided and control release of therapeutics, and bone regeneration scaffolds that promote osteogenesis while allowing magnetic stimulation to enhance healing (Abdel-Hameed et al., 2014; Anand et al., 2023; Marghussian, 2015; Sandu et al., 2012). These multifunctional capabilities make magnetic glass-ceramics attractive materials for medical treatments that require localized and controlled heating, a non-invasive strategy for treating tumors, improving regenerative outcomes, and enabling combined diagnostic and therapeutic functions.

2. Materials and method

2.1 Materials

The magnetic glass-ceramics were synthesized using the following reagents: tetraethyl orthosilicate (TEOS) (Sigma-Aldrich), triethyl phosphate (TEP) (Sigma-Aldrich), calcium nitrate tetrahydrate ($Ca(NO_3)_2{\cdot}4H_2O$) (FAGALAB), distilled water (H_2O) (Jalmek), ethanol (C_2H_5OH) (Jalmek), and nitric acid (HNO_3) (Analytyka), iron chloride hexahydrate ($FeCl_3{\cdot}6H_2O$) (FAGALAB), magnesium nitrate hexahydrate ($(MgNO_3)_2{\cdot}6H_2O$) (Analytyka), citric acid ($C_6H_8O_7{\cdot}H_2O$) (CTR), ethylene glycol ($C_2H_6O_2$) (Analytyka), all analytical grade.

2.2 Synthesis of magnetic glass-ceramics

The glass-ceramics were synthesized using the sol-gel technique. As a first step, the hydrolysis of the organic precursors TEOS and TEP was carried out in solution A, whereas calcium nitrate underwent hydrolysis in solution B. Following this, a mixture of the two solutions resulted in the formation of solution C. Prior to the synthesis process of the glass-ceramic, magnesium ferrite nanoparticles were synthesized via the sol-gel method (De Hoyos-Sifuentes et al., 2022), and these ferrites were incorporated into solution C in 5, 10, 15, and 20 wt%. This solution was subjected to stirring for one hour for gel formation, followed by an aging and drying process. The resulting precursor was subsequently heat-treated at 800 °C under an air atmosphere to induce the formation of the magnetic glass-ceramic.

2.3 Characterization of magnetic glass-ceramics

Phase identification in the material was performed using a Bruker D8 Advance X-ray diffractometer (XRD), employing Cu Kα radiation (λ = 1.54060 Å), with a 2θ scan range from 20° to 70° and a step size of 0.0196°. The data-acquisition rate was approximately 1.67 steps per second. Eva software package from Bruker was used to carry out a detailed analysis of the collected diffraction patterns, providing information on the crystalline phases present in the sample. The structural information of the magnetic glass-ceramics was analyzed using Frontier FT-IR/NIR spectrometer, over the 400–4000 cm^{-1} range at a temperature of 25 °C. The evaluation of magnetic properties was performed using a Quantum Design 6000 vibrating sample magnetometer (VSM), the analysis was performed at temperature of 25 °C, using a constant magnetic field of ±20 kOe. Morphology, particle size and diffraction patterns were analyzed using FEI Titan 80-300 transmission electron microscopy (TEM) equipment.

3. Result and discussion

3.1 X-ray diffraction (XRD)

Figure 1 shows the diffraction patterns of the magnetic glass-ceramics containing 5, 10, 15, and 20 wt% magnesium ferrites, heat treated at 800°C. The diffractograms reveal the characteristic peaks of the hydroxyapatite and inverse spinel structure of magnesium ferrite. At 5% of magnesium ferrite addition, the

patterns exhibit signals characteristic of an amorphous material at lower 2θ angles (Goudouri et al., 2009), along with more defined peaks associated with the (211) and (300) planes of the hydroxyapatite phase (PDF 09-0432).

During thermal treatment, calcium and phosphate ions are released, which are essential for the formation of the hydroxyapatite phase. Additionally, intense peaks associated with the crystallographic planes (220), (311), (400), (511), and (440) corresponding to magnesium ferrite (ICDD:04-008-2382) are identified. As the percentage of magnesium ferrite increases in the samples, there is a notable increase in the amount of this phase, accompanied by a reduction in the hydroxyapatite phase and the amorphous nature of the diffraction pattern. This indicates that magnesium ferrite acts as a glass modifier, inducing significant changes in the crystallization process and the structural properties of the glass-ceramic (Borges et al., 2022).

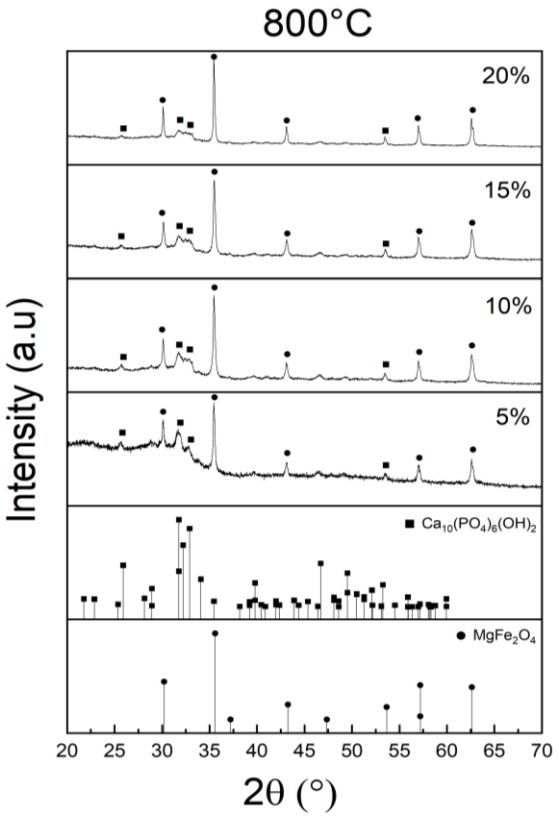

Figure 1. *Diffraction patterns of magnetic glass-ceramics with 5, 10, 15, and 20% $MgFe_2O_4$ at 800 °C.*

3.2 Fourier Transform Infrared Spectroscopy (FTIR)

Figure 2 shows the infrared spectra corresponding to the samples with 5, 10, 15, and 20% magnesium ferrite subjected to heat treatment at 800°C. The spectra reveal the presence of bands between 1065 and 928 cm^{-1} associated with Si-O-Si bonds, confirming the presence of residual amorphous material in the samples. Additionally, phosphate groups were identified, related to the peak at 601 cm^{-1}, which is assigned to the crystalline phase of hydroxyapatite (Ghaebi Panah et al., 2021). Finally, peaks around 422 cm^{-1} were identified as characteristic of the magnesium ferrite structure (Shahjuee et al., 2019). These results corroborate the composition, and the presence of phases identified in the X-ray diffraction analyses.

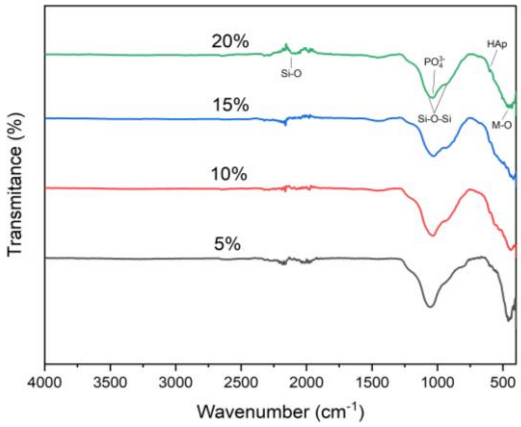

Figure 2. *FTIR of magnetic glass-ceramics with 5, 10, 15, and 20% $MgFe_2O_4$ at 800 °C.*

3.3 Vibrating Sample Magnetometry (VSM)

Figure 3 presents the hysteresis loops obtained from the analysis of the magnetic properties of the glass-ceramics with different percentages of magnesium ferrite (5%, 10%, 15%, and 20%), as well as pure magnesium ferrite ($MgFe_2O_4$). The curves exhibit characteristics typical of soft magnetic materials, evidenced by their sigmoidal shape, low coercivity, and near-zero remanence (B. D. Cullity, 2008), indicative of behavior suitable for use in magnetic hyperthermia.

The results show an increase in saturation magnetization (Ms) proportional to the increase in magnesium ferrite concentration in the glass-ceramics. The Ms of the samples were 1.90 emu/g for 5%, 2.64 emu/g for 10%, 5.69 emu/g for 15% and 7.95 emu/g for 20%. This behavior is attributed to the greater amount of magnetic material present in the glass matrix, confirming the role of magnesium ferrite as the magnetic phase responsible for the observed properties (Poddar et al., 2022).

On the other hand, pure magnesium ferrite exhibits a saturation magnetization of 17.10 emu/g, significantly higher than that of glass-ceramics. This difference can be explained by the dispersion of the magnetic phase within the glass matrix and potential interactions between the phases present. Nonetheless, the results highlight the contribution of magnesium ferrite to the magnetic properties of the glass-ceramics, modulating their magnetic response according to the percentage of ferrite added.

Although saturation magnetization (Ms) is often cited as a key parameter for magnetic hyperthermia, a high Ms alone does not guarantee superior heating efficiency. Heat generation also depends on factors such as particle size and distribution, applied field strength, and mechanisms like eddy currents and Néel–Brown relaxation. For example, (Borges et al., 2022) reported an Ms of approximately 4 emu/g, and (Luderer et al., 1983) an Ms of about 8.7 emu/g both achieving temperatures near 40 °C. These findings demonstrate that hyperthermia efficiency arises from multiple variables, underscoring the potential of our materials for such applications.

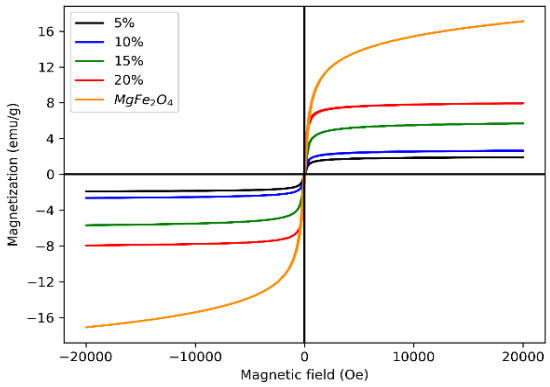

Figure 3. *Hysteresis loops of $MgFe_2O_4$ and magnetic glass-ceramics with 5, 10, 15, and 20% $MgFe_2O_4$ at 800 °C.*

3.4 Transmission electron microscopy

Figure 4 shows the TEM, high-resolution TEM (HRTEM) micrographs, selected area electron diffraction (SAED) patterns, and particle size distribution histograms corresponding to the magnetic glass-ceramic with 20% magnesium ferrite.

In micrograph 4A, the magnesium ferrite nanoparticles are observed as darker regions, as they scatter electrons more effectively compared to hydroxyapatite and glass (Hurley et al., 2015). The particles exhibit spherical morphologies, and form agglomerates due to the intense magnetic interactions characteristic of nanoscale particles (Yeap et al., 2017).

Figure 4B shows the selected area diffraction patterns revealing diffraction spots corresponding to the crystallographic plane (2 2 0) of magnesium ferrite and the plane (3 0 0) hydroxyapatite. The consistent intensity and number of spots indicate high crystallinity.

Figure 4C presents the HRTEM-SAED analysis, highlighting two zones: In the yellow area, diffraction spots corresponding to an interplanar spacing of 2.09 Å were observed. These spots can be indexed to the theoretical interplanar distance of the (400) crystallographic plane, as reported by (Joughehdoust & Manafi, 2012). This observation corroborates one of the characteristic diffraction peaks of magnesium ferrite and confirms the presence of a well-ordered crystalline phase embedded within the glass-ceramic matrix.

In contrast, the red region exhibits a marked absence of diffraction spots, which is attributed to the absence of long-range crystallographic order necessary for electron diffraction. This finding suggests that the glass in this specific area remains in an amorphous state (Hench, 2000). Such behavior underscores the coexistence of the amorphous 58S glass phase and the crystalline magnesium ferrite phase within the sample.

Figure 4D presents the particle size distribution histogram, derived from the measurement of 100 individual particles. The particle sizes range from 1 to 15 nm, with a higher incidence in the range of 4 to 6 nm. The recorded average particle size was 6.10 nm (Predescu et al., 2018).

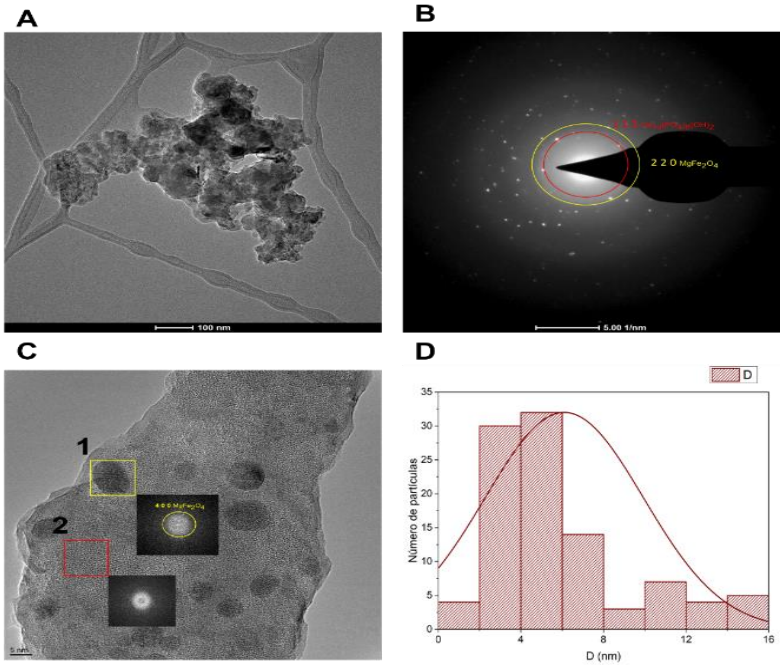

Figure 4. *TEM, HRTEM, SAED and histogram of particle size distribution of magnetic glass-ceramics with 20% of $MgFe_2O_4$ at 800 °C.*

4. Conclusion

The magnetic glass-ceramics were prepared via the sol-gel synthesis route. The resulting materials demonstrated soft magnetic characteristics, with the highest saturation magnetization value of 7.95 emu/g observed in the samples containing 20% magnesium ferrite. TEM analysis revealed optimal particle size distribution with spherical nanoparticles and an average size of 6.1 nm, while XRD and FTIR analyses confirmed the presence of the crystalline phases of $MgFe_2O_4$ and hydroxyapatite.

Glass-ceramics with $MgFe_2O_4$ as the magnetic phase demonstrate a remarkable combination of magnetic and bioactive properties, making them promising candidates for applications in magnetic hyperthermia therapy and bone regeneration.

5. Acknowledgements

This research has been supported by the Tecnológico Nacional de México through the research academic group ITSAL-CA-12 and the research project 21880.25P. Author Diego H. de Hoyos Sifuentes with CVU 998255 is indebted to SECIHTI for financial support in the form of a scholarship for doctorate studies.

6. References

Abdel-Hameed, S. A. M. M., El-Kady, A. M., & Marzouk, M. A. (2014). Magnetic glass ceramics for sustained 5-fluorouracil delivery: Characterization and evaluation of drug release kinetics. *Materials Science and Engineering C*, *44*, 293–309. https://doi.org/10.1016/j.msec.2014.08.022

Anand, V., Chaudhary, A., Meenakshi, Bhatia, G., Heera, P., & Thakur, S. (2023). Magnetic biomaterials with nanostructures for improved medication delivery and bone regeneration. First-level investigation. *Journal of Asian Ceramic Societies*, *11*(4), 526–534. https://doi.org/10.1080/21870764.2023.2251245

B. D. Cullity, C. D. G.-. (2008). *Introduction to magnetic materials*.

Borges, R., Ferreira, L. M., Rettori, C., Lourenço, I. M., Seabra, A. B., Muller, F. A., Ferraz, E. P., Marques, M. M., Miola, M., Baino, F., Mamani, J. B., Gamarra, L. F., & Marchi, J. (2022). Superparamagnetic and highly bioactive SPIONS/bioactive glass nanocomposite and its potential application in magnetic hyperthermia. *Materials Science and Engineering: C*, *March 2021*, 112655. https://doi.org/10.1016/j.msec.2022.112655

De Hoyos-Sifuentes, D. H., Reséndiz-Hernández, P. J., Díaz-Guillén, J. A., Ochoa-Palacios, R. M., & Altamirano-Guerrero, G. (2022). Synthesis and characterization of MgFe2O4nanoparticles and PEG-coated MgFe2O4nanocomposite. *Journal of Materials Research and Technology*, *18*, 3130–3142. https://doi.org/10.1016/j.jmrt.2022.03.117

Díez-Tercero, L., Delgado, L. M., Bosch-Rué, E., & Perez, R. A. (2021). Evaluation of the immunomodulatory effects of cobalt, copper and magnesium ions in a pro inflammatory environment. *Scientific Reports*, *11*(1), 1–13. https://doi.org/10.1038/s41598-021-91070-0

Farid, S. B. H. H. (2019). *Bioceramics: For Materials Science and Engineering* (Vol. 1).

Ghaebi Panah, N., Atkin, R., & Sercombe, T. B. (2021). Effect of low temperature crystallization on 58S bioactive glass

sintering and compressive strength. *Ceramics International*, *47*(21), 30349–30357. https://doi.org/10.1016/j.ceramint.2021.07.215

Goudouri, O. M., Chatzistavrou, X., Kontonasaki, E., Kantiranis, N., Papadopoulou, L., Chrissafis, K., & Paraskevopoulos, K. M. (2009). Study of the bioactive behavior of thermally treated modified 58S bioactive glass. *Key Engineering Materials*, *396–398*, 131–134. https://doi.org/10.4028/www.scientific.net/kem.396-398.131

Hench, L. L. (2000). (ii) The challenge of orthopaedic materials. *Current Orthopaedics*, *14*(1), 7–15. https://doi.org/10.1054/cuor.1999.0074

Hench, L. L. (2006). The story of Bioglass®. *Journal of Materials Science: Materials in Medicine*, *17*(11), 967–978. https://doi.org/10.1007/s10856-006-0432-z

Hurley, K. R., Ring, H. L., Kang, H., Klein, N. D., & Haynes, C. L. (2015). Characterization of Magnetic Nanoparticles in Biological Matrices. *Analytical Chemistry*, *87*(23), 11611–11619. https://doi.org/10.1021/acs.analchem.5b02229

Joughehdoust, S., & Manafi, S. (2012). Synthesis and in vitro investigation of sol-gel derived bioglass-58S nanopowders. *Materials Science-Poland*, *30*(1), 45–52. https://doi.org/10.2478/s13536-012-0007-2

Kaou, M. H., Furkó, M., Balázsi, K., & Balázsi, C. (2023). Advanced Bioactive Glasses: The Newest Achievements and Breakthroughs in the Area. *Nanomaterials*, *13*(16), 1–33. https://doi.org/10.3390/nano13162287

Luderer, A. A., Borrelli, N. F., Panzarino, J. N., Mansfield, G. R., Hess, D. M., Brown, J. L., Barnett, E. H., & Hahn, E. W. (1983). Glass-ceramic-mediated, magnetic-field-induced localized hyperthermia: Response of a murine mammary carcinoma. *Radiation Research*, *94*(1), 190–198. https://doi.org/10.2307/3575874

Marghussian, V. (2015). Magnetic Properties of Nano-Glass Ceramics. In *Nano-Glass Ceramics*. Elsevier. https://doi.org/10.1016/b978-0-323-35386-1.00004-9

Poddar, A., Halder, S., Liba, S. I., Hoque, S. M., & Sikder, S. S. (2022). Study of the Effect of Quenching on Microstructural and Magnetic Properties of Cu-Doped Mg-Ferrite. *Advances in Condensed Matter Physics*, *2022*. https://doi.org/10.1155/2022/3354087

Predescu, A. M., Matei, E., Berbecaru, A. C., Pantilimon, C., Drăgan, C., Vidu, R., Predescu, C., & Kuncser, V. (2018). Synthesis and characterization of dextran-coated iron oxide nanoparticles. *Royal Society Open Science*, *5*(3). https://doi.org/10.1098/rsos.171525

Sandu, V., Kuncser, V., Damian, R., & Sandu, E. (2012). *Magnetic glass-ceramics*. *1*(2), 138–143. https://doi.org/10.1007/s40145-012-0010-4

Shahjuee, T., Masoudpanah, S. M., & Mirkazemi, S. M. (2019). Thermal Decomposition Synthesis of MgFe2O4 Nanoparticles for Magnetic Hyperthermia. *Journal of Superconductivity and Novel Magnetism*, *32*(5), 1347–1352. https://doi.org/10.1007/s10948-018-

4834-1

Shearer, A., Montazerian, M., & Mauro, J. C. (2023). Modern definition of bioactive glasses and glass-ceramics. *Journal of Non-Crystalline Solids*, *608*, 1–20. https://doi.org/10.1016/j.jnoncrysol.2023.122228

Thompson, Z., Rahman, S., Yarmolenko, S., Sankar, J., Kumar, D., & Bhattarai, N. (2017). Fabrication and characterization of magnesium ferrite-based PCL/Aloe vera nanofibers. *Materials*, *10*(8), 1–12. https://doi.org/10.3390/ma10080937

Yeap, S. P., Lim, J. K., Ooi, B. S., & Ahmad, A. L. (2017). Agglomeration, colloidal stability, and magnetic separation of magnetic nanoparticles: collective influences on environmental engineering applications. *Journal of Nanoparticle Research*, *19*(11). https://doi.org/10.1007/s11051-017-4065-6

Zhu, Y., Zhang, X., Chang, G., Deng, S., & Chan, H. F. (2024). Bioactive Glass in Tissue Regeneration: Unveiling Recent Advances in Regenerative Strategies and Applications. *Advanced Materials*, *2312964*, 1–16. https://doi.org/10.1002/adma.202312964